

Hybrid Particle-Field Molecular Dynamics Under Constant Pressure

Sigbjørn Løland Bore¹, Giuseppe Milano² and Michele Cascella¹

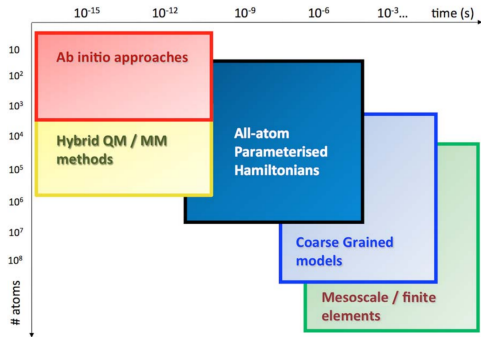
¹Hylleraas Centre for Quantum Molecular Sciences,
Department of Chemistry, University of Oslo, Norway

²Department of Organic Materials Science, Yamagata University, Japan

NKS Annual Meeting, Trondheim, 9 October 2019

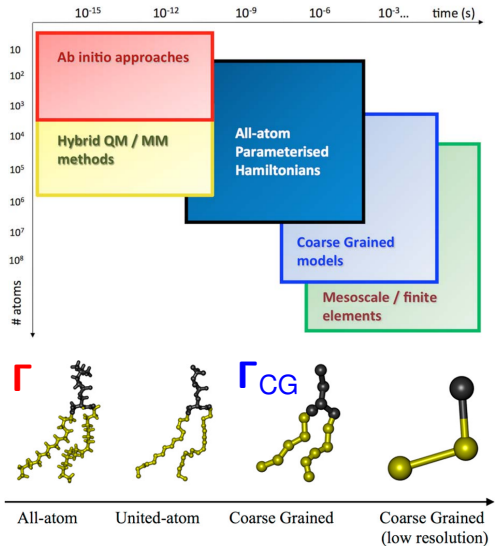


Coarse-graining

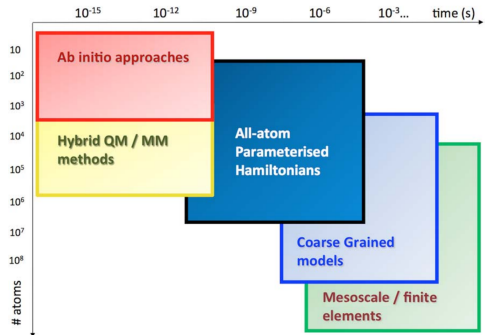


*M. Cascella and S. Vanni, Chem. Modell., (2016), 12
T. A. Soares, et al., J. Phys. Chem. Lett., (2017) 8(15)*

Coarse-graining

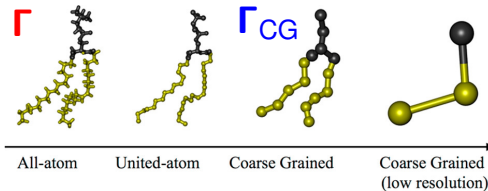


Coarse-graining



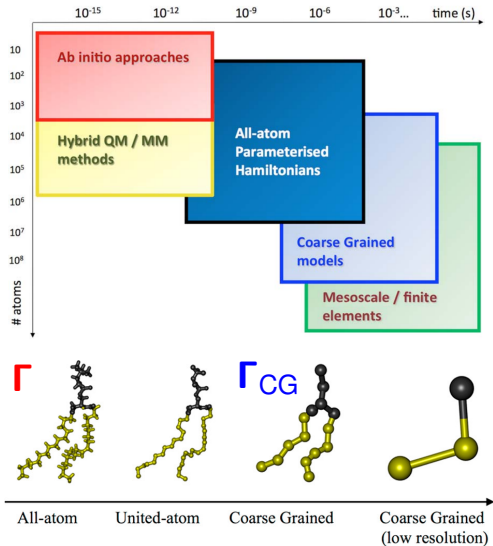
$$Z = \int d\Gamma e^{-\beta H(\Gamma)}$$

$$Z \simeq \int d\Gamma_{CG} e^{-\beta H(\Gamma_{CG})}$$



*M. Cascella and S. Vanni, Chem. Modell., (2016), 12
T. A. Soares, et al., J. Phys. Chem. Lett., (2017) 8(15)*

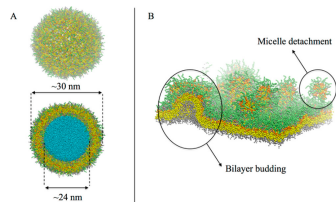
Coarse-graining



$$Z = \int d\Gamma e^{-\beta H(\Gamma)}$$

↓

$$Z \simeq \int d\Gamma_{CG} e^{-\beta H(\Gamma_{CG})}$$



Large systems and
long time scales

The Hybrid Particle-field method

$$H(\{\mathbf{r}\}) = \sum_{m=1}^{N_{\text{mol}}} \underbrace{H_0(\{\mathbf{r}_m\})}_{\text{Intra-molecular}} + \underbrace{W[\{\phi(\mathbf{r})\}]}_{\text{Inter-molecular}}$$

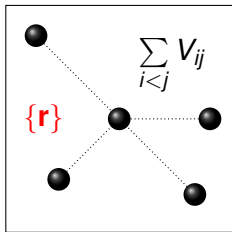
$\{\phi\} \equiv \{\phi_1, \dots, \phi_M\}$, particle-type number densities.

The Hybrid Particle-field method

$$H(\{\mathbf{r}\}) = \sum_{m=1}^{N_{\text{mol}}} \underbrace{H_0(\{\mathbf{r}_m\})}_{\text{Intra-molecular}} + \underbrace{W[\{\phi(\mathbf{r})\}]}_{\text{Inter-molecular}}$$

Intermolecular interactions

Particle-particle



$\{\mathbf{r}\} \equiv \{\mathbf{r}_1, \dots, \mathbf{r}_N\}$, *particle positions*.

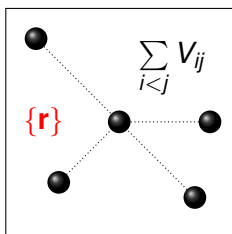
$\{\phi\} \equiv \{\phi_1, \dots, \phi_M\}$, *particle-type number densities*.

The Hybrid Particle-field method

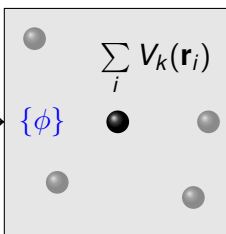
$$H(\{\mathbf{r}\}) = \sum_{m=1}^{N_{\text{mol}}} \underbrace{H_0(\{\mathbf{r}_m\})}_{\text{Intra-molecular}} + \underbrace{W[\{\phi(\mathbf{r})\}]}_{\text{Inter-molecular}}$$

Intermolecular interactions

Particle-particle



Particle-field



$\{\mathbf{r}\} \equiv \{\mathbf{r}_1, \dots, \mathbf{r}_N\}$, *particle positions*.

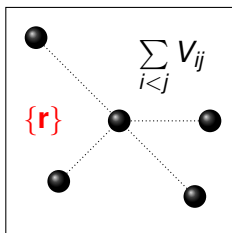
$\{\phi\} \equiv \{\phi_1, \dots, \phi_M\}$, *particle-type number densities*.

The Hybrid Particle-field method

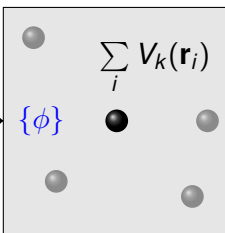
$$H(\{\mathbf{r}\}) = \sum_{m=1}^{N_{\text{mol}}} \underbrace{H_0(\{\mathbf{r}_m\})}_{\text{Intra-molecular}} + \underbrace{W[\{\phi(\mathbf{r})\}]}_{\text{Inter-molecular}}$$

Intermolecular interactions

Particle-particle



Particle-field



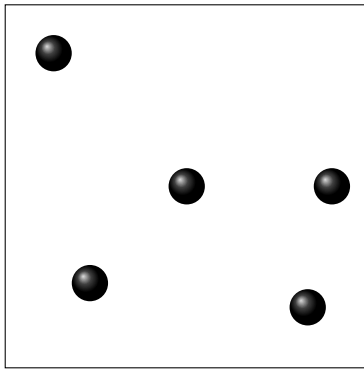
$$V_k(\mathbf{r}) = \frac{\delta W[\{\phi\}]}{\delta \phi_k(\mathbf{r})}$$

$$\mathbf{F}_i = -\nabla_i V_k(\mathbf{r}_i)$$

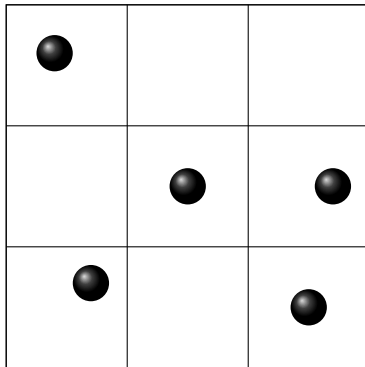
$\{\mathbf{r}\} \equiv \{\mathbf{r}_1, \dots, \mathbf{r}_N\}$, *particle positions*.

$\{\phi\} \equiv \{\phi_1, \dots, \phi_M\}$, *particle-type number densities*.

Force computation: Particle-mesh

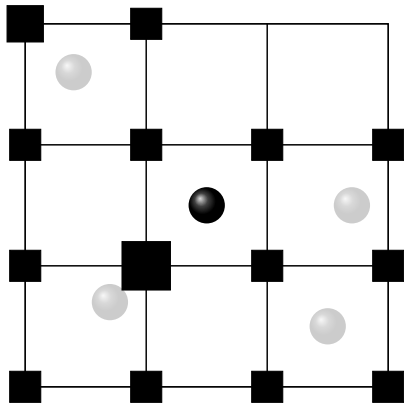


Force computation: Particle-mesh



1) Linear interpolation:
 $\{\mathbf{r}\} \rightarrow \{\phi_{nml}\}$

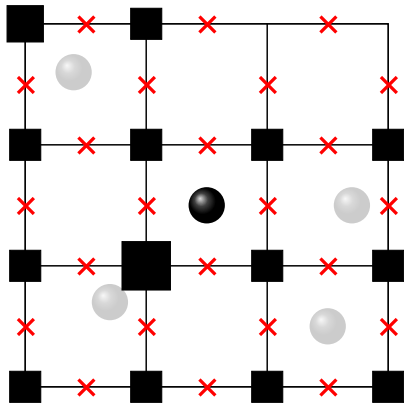
Force computation: Particle-mesh



1) Linear interpolation:
 $\{\mathbf{r}\} \rightarrow \{\phi_{nml}\}$

■ : ϕ_{nml}

Force computation: Particle-mesh



1) Linear interpolation:

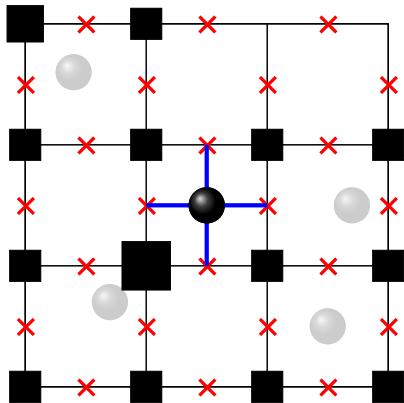
$$\{\mathbf{r}\} \rightarrow \{\phi_{nml}\}$$

2) Finite-differences:

$$\{\phi_{nml}\} \rightarrow \{\nabla \phi_{nml}\} \rightarrow \{\nabla V_{nml}\}$$

■ : ϕ_{nml} ✕ : ∇V_{nml}

Force computation: Particle-mesh



1) Linear interpolation:

$$\{\mathbf{r}\} \rightarrow \{\phi_{nml}\}$$

2) Finite-differences:

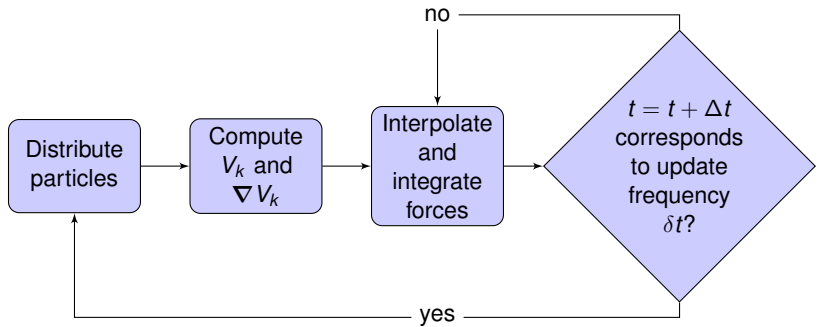
$$\{\phi_{nml}\} \rightarrow \{\nabla \phi_{nml}\} \rightarrow \{\nabla V_{nml}\}$$

3) Force interpolation:

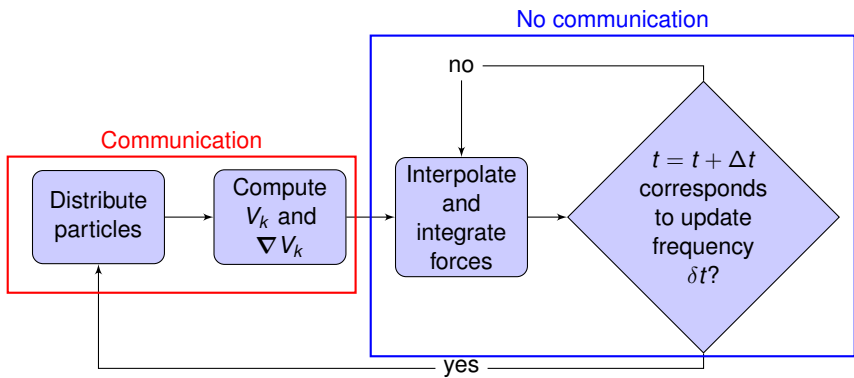
$$\{\nabla V_{nml}\} \rightarrow \mathbf{F}_i$$

■ : ϕ_{nml} ✗ : ∇V_{nml}

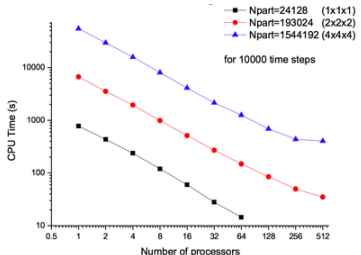
Implementation and parallelization



Implementation and parallelization



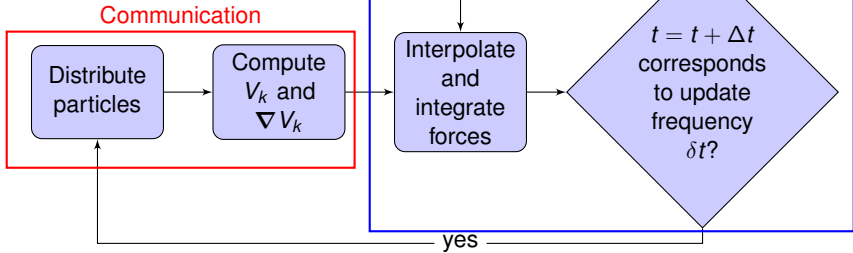
Implementation and parallelization



Excellent scaling for small and large systems!



No communication



Example of $W[\phi]$: Polymer-theory

$$W[\phi] = \int d\mathbf{r} \frac{1}{\rho_0} \left(\sum_{k\ell} \frac{\tilde{\chi}_{k\ell}}{2} \phi_k(\mathbf{r}) \phi_\ell(\mathbf{r}) + \frac{1}{\kappa} \left(\sum_\ell \phi_\ell(\mathbf{r}) - a \right)^2 \right)$$

(ρ_0 : density-parameter related to the volume per bead.
 a : equation of state parameter.)

Example of $W[\phi]$: Polymer-theory

$$W[\phi] = \int d\mathbf{r} \frac{1}{\rho_0} \left(\underbrace{\sum_{k\ell} \frac{\tilde{\chi}_{k\ell}}{2} \phi_k(\mathbf{r}) \phi_\ell(\mathbf{r})}_{\text{Mixing}} + \frac{1}{\kappa} \left(\sum_\ell \phi_\ell(\mathbf{r}) - a \right)^2 \right)$$

$\tilde{\chi}_{k\ell} > 0 \rightarrow$ Likes not to mix

$\tilde{\chi}_{k\ell} \leq 0 \rightarrow$ Likes to mix

(ρ_0 : density-parameter related to the volume per bead.
 a : equation of state parameter.)

Example of $W[\phi]$: Polymer-theory

$$W[\phi] = \int d\mathbf{r} \frac{1}{\rho_0} \left(\underbrace{\sum_{k\ell} \frac{\tilde{\chi}_{k\ell}}{2} \phi_k(\mathbf{r}) \phi_\ell(\mathbf{r})}_{\text{Mixing}} + \underbrace{\frac{1}{\kappa} \left(\sum_\ell \phi_\ell(\mathbf{r}) - a \right)^2}_{\text{Compressibility}} \right)$$

$\tilde{\chi}_{k\ell} > 0 \rightarrow$ Likes not to mix

$\kappa \sim 0 \rightarrow$ incompressible

$\tilde{\chi}_{k\ell} \leq 0 \rightarrow$ Likes to mix

$\kappa \gg 0 \rightarrow$ very compressible

(ρ_0 : density-parameter related to the volume per bead.
 a : equation of state parameter.)

Example of $W[\phi]$: Polymer-theory

$$W[\phi] = \int d\mathbf{r} \frac{1}{\rho_0} \left(\underbrace{\sum_{k\ell} \frac{\tilde{\chi}_{k\ell}}{2} \phi_k(\mathbf{r}) \phi_\ell(\mathbf{r})}_{\text{Mixing}} + \underbrace{\frac{1}{\kappa} \left(\sum_\ell \phi_\ell(\mathbf{r}) - a \right)^2}_{\text{Compressibility}} \right)$$

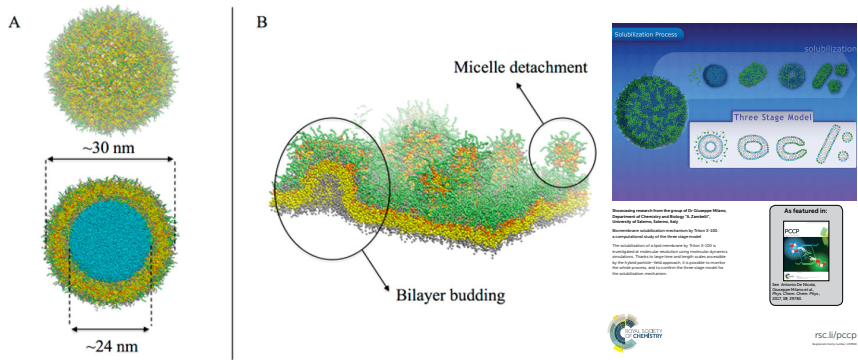
$\tilde{\chi}_{k\ell} > 0 \rightarrow$ Likes not to mix $\kappa \sim 0 \rightarrow$ incompressible
 $\tilde{\chi}_{k\ell} \leq 0 \rightarrow$ Likes to mix $\kappa \gg 0 \rightarrow$ very compressible

$$\frac{\delta W[\{\phi\}]}{\delta \phi_k(\mathbf{r})} \xrightarrow{\text{Net effect}} V_k(\mathbf{r}) = \frac{1}{\rho_0} \left(\sum_\ell \tilde{\chi}_{k\ell} \phi_\ell(\mathbf{r}) + \frac{1}{\kappa} \left(\sum_\ell \phi_\ell(\mathbf{r}) - a \right) \right)$$

(ρ_0 : density-parameter related to the volume per bead.
 a : equation of state parameter.)

Prototypic application

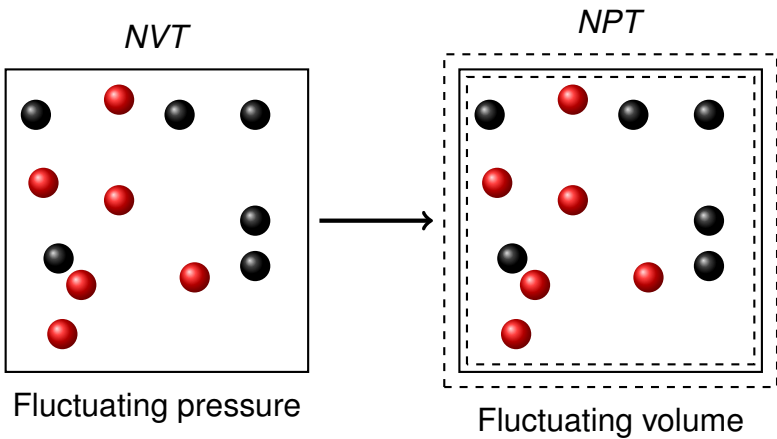
Large lipid vesicles interacting with surfactants



T. A. Soares *et al.*, *JPCL* 2017

A. Pizzirusso *et al.*, *PCCP* 2017

Extension to constant pressure simulation



Pressure from thermodynamics

From the Helmholtz free energy:

$$P = - \left(\frac{\partial F}{\partial V} \right)_{T,N}$$

Pressure from thermodynamics

From the Helmholtz free energy:

$$P = - \left(\frac{\partial F}{\partial V} \right)_{T,N}$$

Use definition of partition function:

$$P = - \frac{\partial}{\partial V} \frac{1}{\beta} \ln Q(V, T) = - \frac{\partial}{\partial V} \frac{1}{\beta} \ln \left[\int \frac{d\mathbf{r}^N}{V^N} d\mathbf{p}^N \, V^N e^{-\beta(K+U)} \right].$$

Pressure from thermodynamics

From the Helmholtz free energy:

$$P = - \left(\frac{\partial F}{\partial V} \right)_{T,N}$$

Use definition of partition function:

$$P = - \frac{\partial}{\partial V} \frac{1}{\beta} \ln Q(V, T) = - \frac{\partial}{\partial V} \frac{1}{\beta} \ln \left[\int \frac{d\mathbf{r}^N}{V^N} d\mathbf{p}^N \, V^N e^{-\beta(K+U)} \right].$$

Compute the derivative:

$$P = \frac{1}{3V} \left(3k_b T - \left\langle V \frac{\partial U}{\partial V} \right\rangle_{T,N} \right)$$

($\beta \equiv 1/k_b T$, U : potential energy, K : kinetic energy)

Pressure in molecular dynamics

Generalization to multiple components:

$$P_\mu = \frac{1}{V} \left(2 \langle K_\mu \rangle - \left\langle L_\mu \frac{\partial U}{\partial L_\mu} \right\rangle_{T,N} \right)$$

(L_μ : sidelengths of box. μ : components xx , yy and zz . $\mathbf{r}_{ij} \equiv \mathbf{r}_i - \mathbf{r}_j$.)

Pressure in molecular dynamics

Generalization to multiple components:

$$P_\mu = \frac{1}{V} \left(2 \langle K_\mu \rangle - \left\langle L_\mu \frac{\partial U}{\partial L_\mu} \right\rangle_{T,N} \right)$$

Forces on particles:

$$P_\mu = \frac{1}{V} \left(2 \langle K_\mu \rangle - \sum_{i=1}^N \left\langle \frac{\partial U}{\partial r_{\mu,i}} \cdot \mathbf{r}_{\mu,i} \right\rangle_{T,N} \right), \quad \text{Dependent on origo}$$

(L_μ : sidelengths of box. μ : components xx , yy and zz . $\mathbf{r}_{ij} \equiv \mathbf{r}_i - \mathbf{r}_j$.)

Pressure in molecular dynamics

Generalization to multiple components:

$$P_\mu = \frac{1}{V} \left(2 \langle K_\mu \rangle - \left\langle L_\mu \frac{\partial U}{\partial L_\mu} \right\rangle_{T,N} \right)$$

Forces on particles:

$$P_\mu = \frac{1}{V} \left(2 \langle K_\mu \rangle - \sum_{i=1}^N \left\langle \frac{\partial U}{\partial r_{\mu,i}} \cdot \mathbf{r}_{\mu,i} \right\rangle_{T,N} \right), \quad \text{Dependent on origo}$$

Pair interactions N particles:

$$P_\mu = \frac{1}{V} \left(2 \langle K_\mu \rangle - \sum_{i < j}^N \left\langle \frac{\partial U}{\partial \mathbf{r}_{\mu,ij}} \cdot \mathbf{r}_{\mu,ij} \right\rangle_{T,N} \right), \quad \text{Independent on origo}$$

(L_μ : sidelengths of box. μ : components xx , yy and zz . $\mathbf{r}_{ij} \equiv \mathbf{r}_i - \mathbf{r}_j$.)

Pressure for particle-field

Hybrid particle field interaction-energy:

$$W_0[\phi] = \int d\mathbf{r} \frac{1}{\rho_0} \left(\sum_{k\ell} \frac{\tilde{\chi}_{k\ell}}{2} \phi_k(\mathbf{r}) \phi_\ell(\mathbf{r}) + \frac{1}{\kappa} \left(\sum_\ell \phi_\ell(\mathbf{r}) - a \right)^2 \right)$$

(a : equation of state parameter.)

Pressure for particle-field

Hybrid particle field interaction-energy:

$$W_0[\phi] = \int d\mathbf{r} \frac{1}{\rho_0} \left(\sum_{k\ell} \frac{\tilde{\chi}_{k\ell}}{2} \phi_k(\mathbf{r}) \phi_\ell(\mathbf{r}) + \frac{1}{\kappa} \left(\sum_\ell \phi_\ell(\mathbf{r}) - a \right)^2 \right)$$

No pair interactions, but we can use $P_\mu = -\frac{1}{V} \left\langle L_\mu \frac{\partial W}{\partial L_\mu} \right\rangle_{T,N}$:

(a : equation of state parameter.)

Pressure for particle-field

Hybrid particle field interaction-energy:

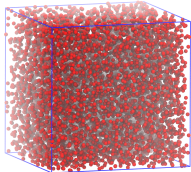
$$W_0[\phi] = \int d\mathbf{r} \frac{1}{\rho_0} \left(\sum_{k\ell} \frac{\tilde{\chi}_{k\ell}}{2} \phi_k(\mathbf{r}) \phi_\ell(\mathbf{r}) + \frac{1}{\kappa} \left(\sum_\ell \phi_\ell(\mathbf{r}) - a \right)^2 \right)$$

No pair interactions, but we can use $P_\mu = -\frac{1}{V} \left\langle L_\mu \frac{\partial W}{\partial L_\mu} \right\rangle_{T,N}$:

$$P_{0,\mu} = \frac{1}{V} \int d\mathbf{r} \frac{1}{\rho_0} \left(\sum_{k\ell} \frac{\tilde{\chi}_{k\ell}}{2} \phi_k(\mathbf{r}) \phi_\ell(\mathbf{r}) + \frac{1}{2\kappa} \left(\phi(\mathbf{r})^2 - a^2 \right) \right),$$

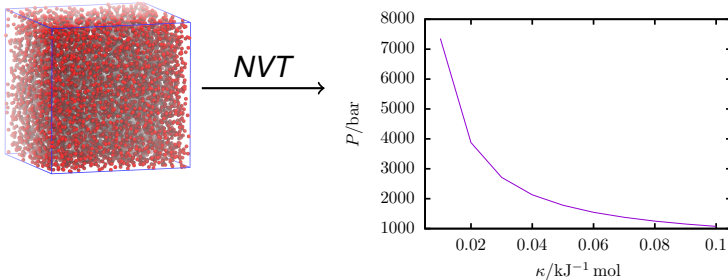
(a : equation of state parameter.)

Single-phase: “Liquid water” at 300 K



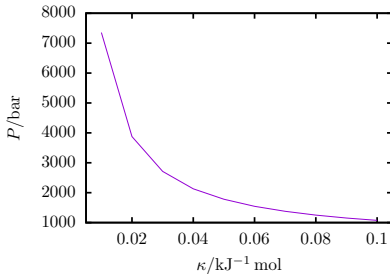
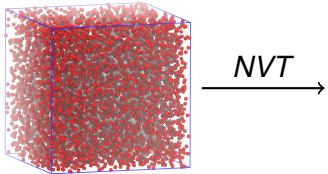
$$P_{0,\mu} = \frac{1}{V} \int d\mathbf{r} \frac{1}{\rho_0} \frac{1}{2\kappa} (\phi(\mathbf{r})^2 - a^2)$$

Single-phase: “Liquid water” at 300 K

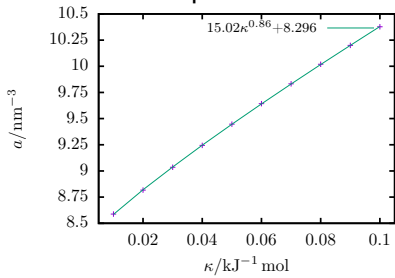


$$P_{0,\mu} = \frac{1}{V} \int d\mathbf{r} \frac{1}{\rho_0} \frac{1}{2\kappa} (\phi(\mathbf{r})^2 - a^2)$$

Single-phase: “Liquid water” at 300 K

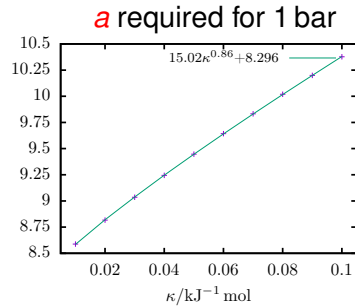
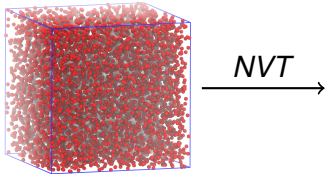


a required for 1 bar

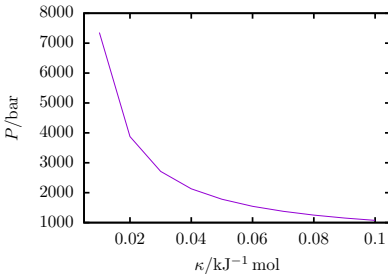


$$P_{0,\mu} = \frac{1}{V} \int d\mathbf{r} \frac{1}{\rho_0} \frac{1}{2\kappa} (\phi(\mathbf{r})^2 - a^2)$$

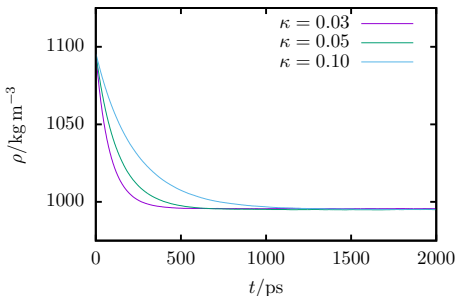
Single-phase: “Liquid water” at 300 K



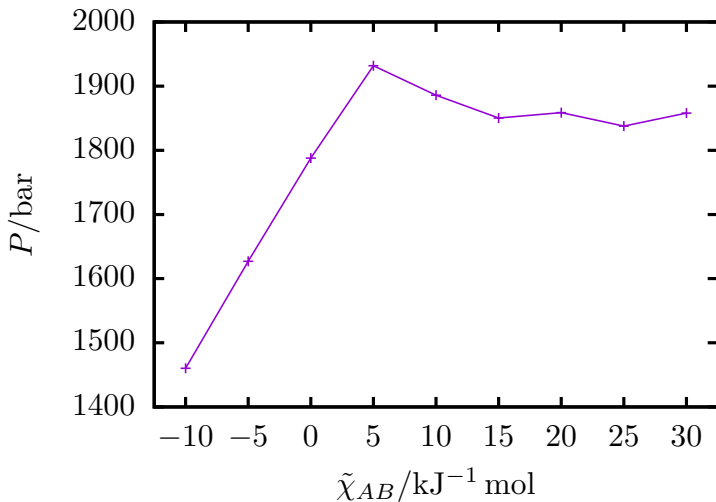
$$P_{0,\mu} = \frac{1}{V} \int d\mathbf{r} \frac{1}{\rho_0} \frac{1}{2\kappa} (\phi(\mathbf{r})^2 - a^2)$$



NPT-equilibration

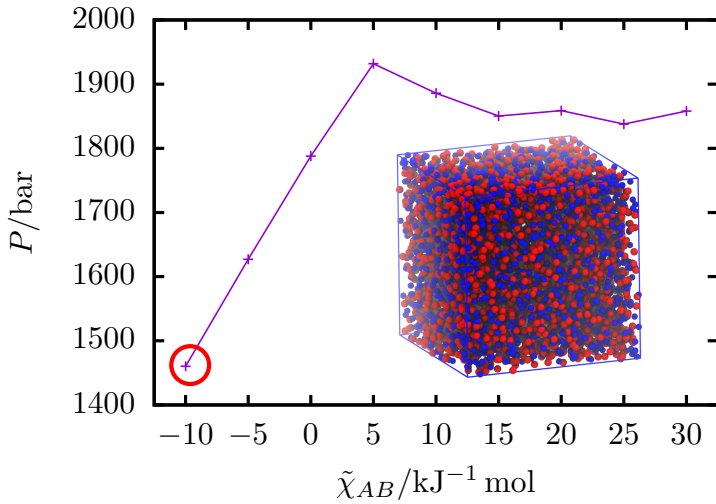


Binary-phase: Effect of miscibility



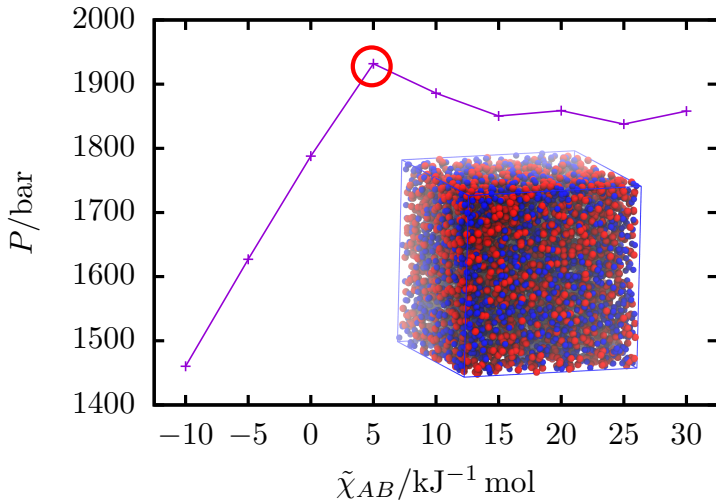
$$P_{0,\mu} = \frac{1}{V} \int d\mathbf{r} \frac{1}{\rho_0} \frac{\tilde{\chi}_{AB}}{2} \phi_A(\mathbf{r}) \phi_B(\mathbf{r})$$

Binary-phase: Effect of miscibility



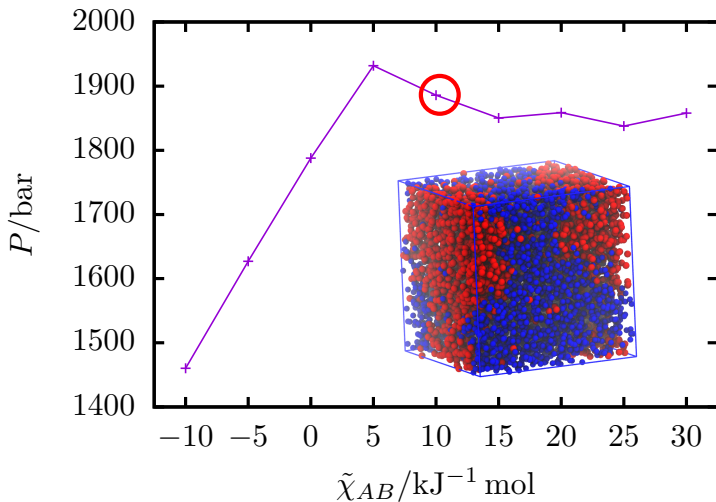
$$P_{0,\mu} = \frac{1}{V} \int d\mathbf{r} \frac{1}{\rho_0} \frac{\tilde{\chi}_{AB}}{2} \phi_A(\mathbf{r}) \phi_B(\mathbf{r})$$

Binary-phase: Effect of miscibility



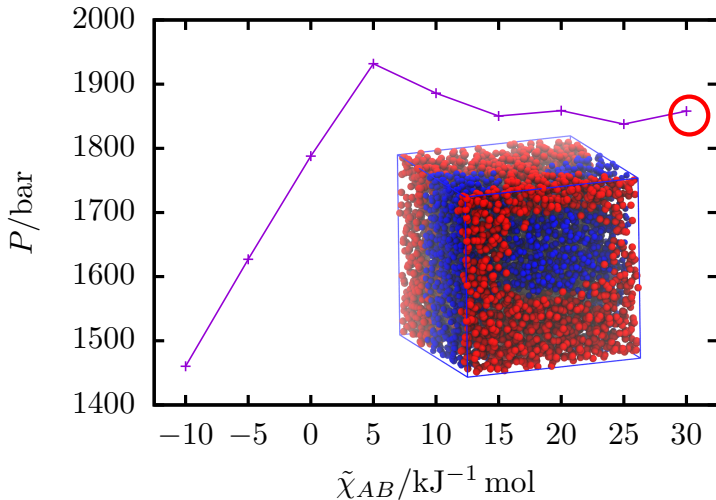
$$P_{0,\mu} = \frac{1}{V} \int d\mathbf{r} \frac{1}{\rho_0} \frac{\tilde{\chi}_{AB}}{2} \phi_A(\mathbf{r}) \phi_B(\mathbf{r})$$

Binary-phase: Effect of miscibility



$$P_{0,\mu} = \frac{1}{V} \int d\mathbf{r} \frac{1}{\rho_0} \frac{\tilde{\chi}_{AB}}{2} \phi_A(\mathbf{r}) \phi_B(\mathbf{r})$$

Binary-phase: Effect of miscibility



$$P_{0,\mu} = \frac{1}{V} \int d\mathbf{r} \frac{1}{\rho_0} \frac{\tilde{\chi}_{AB}}{2} \phi_A(\mathbf{r}) \phi_B(\mathbf{r})$$

Modeling of surface-tension

Hybrid particle field interaction-energy:

$$W_1[\nabla\phi] = \frac{1}{2\rho_0} \sum_{k,\ell} \int d\mathbf{r} K_{k\ell} \nabla\phi_k(\mathbf{r}) \cdot \nabla\phi_\ell(\mathbf{r})$$

Modeling of surface-tension

Hybrid particle field interaction-energy:

$$W_1[\nabla \phi] = \frac{1}{2\rho_0} \sum_{k,\ell} \int d\mathbf{r} K_{k\ell} \nabla \phi_k(\mathbf{r}) \cdot \nabla \phi_\ell(\mathbf{r})$$

Pressure contribution:

$$P_{1,\mu} = \frac{1}{V} \int d\mathbf{r} \sum_{k\ell} \frac{K_{k\ell}}{\rho_0} \left(\frac{1}{2} \nabla \phi_k(\mathbf{r}) \cdot \nabla \phi_\ell(\mathbf{r}) + \nabla_\mu \phi_k(\mathbf{r}) \nabla_\mu \phi_\ell(\mathbf{r}) \right)$$

Modeling of surface-tension

Hybrid particle field interaction-energy:

$$W_1[\nabla \phi] = \frac{1}{2\rho_0} \sum_{k,\ell} \int d\mathbf{r} K_{k\ell} \nabla \phi_k(\mathbf{r}) \cdot \nabla \phi_\ell(\mathbf{r})$$

Pressure contribution:

$$P_{1,\mu} = \frac{1}{V} \int d\mathbf{r} \sum_{k\ell} \frac{K_{k\ell}}{\rho_0} \left(\frac{1}{2} \nabla \phi_k(\mathbf{r}) \cdot \nabla \phi_\ell(\mathbf{r}) + \nabla_\mu \phi_k(\mathbf{r}) \nabla_\mu \phi_\ell(\mathbf{r}) \right)$$

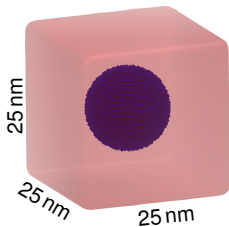
Surface-tension over interface:

$$\gamma = \int dz \sum_{k\ell} \frac{K_{k\ell}}{V\rho_0} (\nabla_\perp \phi_k(\mathbf{r}) \nabla_\perp \phi_\ell(\mathbf{r}) - \nabla_\parallel \phi_k(\mathbf{r}) \nabla_\parallel \phi_\ell(\mathbf{r}))$$

$$(\gamma = \int dz (P_\perp(z) - P_\parallel(z)))$$

Example of surface-tension: Droplet in solvent

Starting configuration



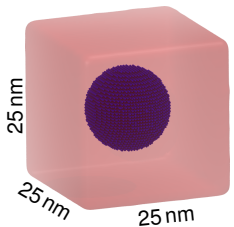
$$\tilde{\chi}_{AB} = 20 \text{ kJ mol}^{-1}$$

$$W_1[\nabla\phi] = \frac{-1}{\rho_0} \int d\mathbf{r} K_{ST} \nabla\phi_A(\mathbf{r}) \cdot \nabla\phi_B(\mathbf{r})$$

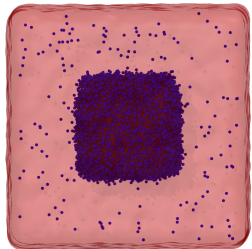
Example of surface-tension: Droplet in solvent

Final configurations

Starting configuration



$$K_{ST} = -2 \text{ kJ nm}^2$$



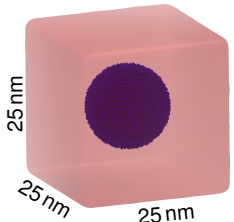
$$\tilde{\chi}_{AB} = 20 \text{ kJ mol}^{-1}$$

$$W_1[\nabla\phi] = \frac{-1}{\rho_0} \int d\mathbf{r} K_{ST} \nabla\phi_A(\mathbf{r}) \cdot \nabla\phi_B(\mathbf{r})$$

Example of surface-tension: Droplet in solvent

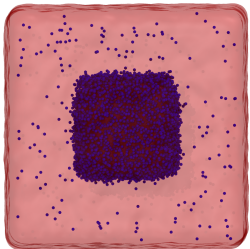
Final configurations

Starting configuration

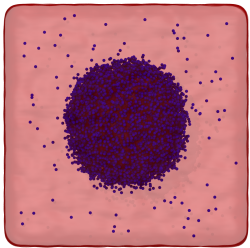


$$\tilde{\chi}_{AB} = 20 \text{ kJ mol}^{-1}$$

$$K_{ST} = -2 \text{ kJ nm}^2$$



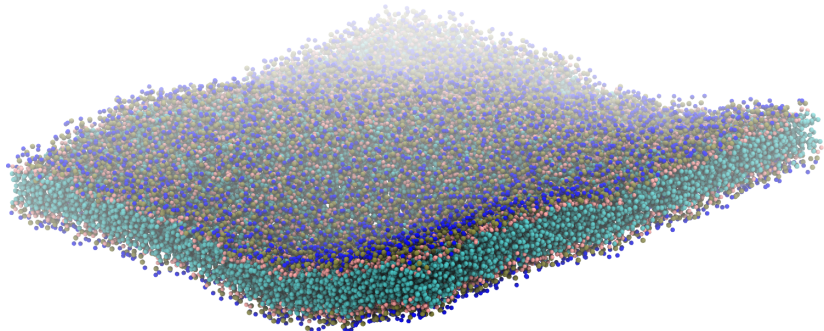
$$K_{ST} = 4 \text{ kJ nm}^2$$



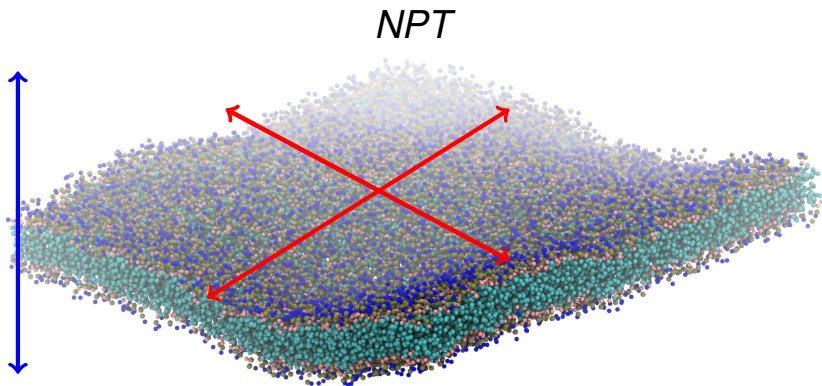
$$W_1[\nabla\phi] = \frac{-1}{\rho_0} \int d\mathbf{r} K_{ST} \nabla\phi_A(\mathbf{r}) \cdot \nabla\phi_B(\mathbf{r})$$

Constant pressure lipid-bilayer simulations

NPT

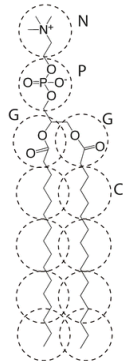


Constant pressure lipid-bilayer simulations



Particle-field model for DPPC phospholipid

Standard model for DPPC:



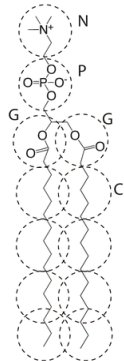
$$H_0 = \sum \frac{m_i v_i^2}{2} + \sum \frac{k_r(r_{ij}-r_0)^2}{2} + \sum \frac{k_\theta(\cos(\theta_{ijk})-\cos(\theta_0))^2}{2}$$

$$W_0 = \frac{1}{2\rho_0} \int d\mathbf{r} \left(\sum_{kl} \tilde{\chi}_{kl} e \phi_k(\mathbf{r}) \phi_l(\mathbf{r}) + \frac{1}{\kappa} \left(\sum_l \phi_l(\mathbf{r}) - a \right)^2 \right)$$

G	P	C	W	
-1.50	6.30	9.00	-8.10	N
	4.50	13.50	-3.60	P
		6.30	4.50	G
$\tilde{\chi}_{kl}/\text{kJ mol}^{-1}$			33.75	C

Particle-field model for DPPC phospholipid

Standard model for DPPC:



$$H_0 = \sum \frac{m_i v_i^2}{2} + \sum \frac{k_r(r_{ij}-r_0)^2}{2} + \sum \frac{k_\theta(\cos(\theta_{ijk})-\cos(\theta_0))^2}{2}$$

$$W_0 = \frac{1}{2\rho_0} \int d\mathbf{r} \left(\sum_{kl} \tilde{\chi}_{kl} e \phi_k(\mathbf{r}) \phi_l(\mathbf{r}) + \frac{1}{\kappa} \left(\sum_l \phi_l(\mathbf{r}) - a \right)^2 \right)$$

	G	P	C	W	
$\tilde{\chi}_{kl}/\text{kJ mol}^{-1}$	-1.50	6.30	9.00	-8.10	N
		4.50	13.50	-3.60	P
			6.30	4.50	G
				33.75	C

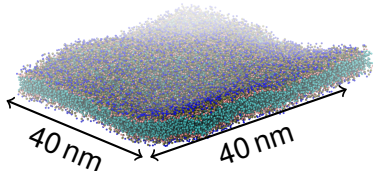
Modeling of tension: $W_1 = -\frac{1}{\rho_0} \int d\mathbf{r} (\mathcal{K}_{ST} \nabla \phi_W(\mathbf{r}) \cdot \nabla \phi_C(\mathbf{r}))$

$\mathcal{K}_{ST} < 0$: *Energy loss for surface area*

$\mathcal{K}_{ST} > 0$: *Energy gain for surface area*

The effect of K_{ST} on DPPC-Bilayer

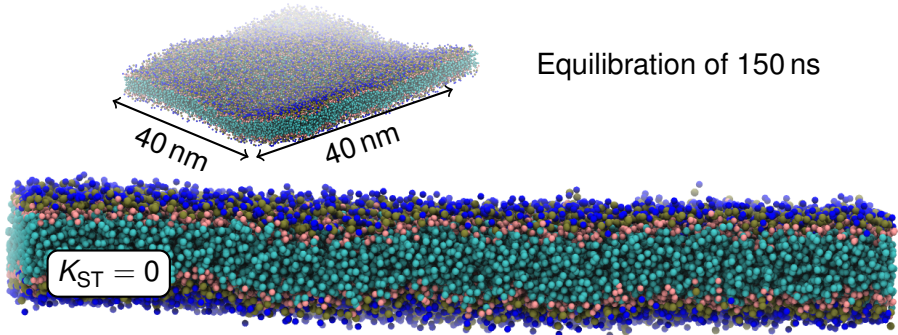
System setup



Equilibration of 150 ns

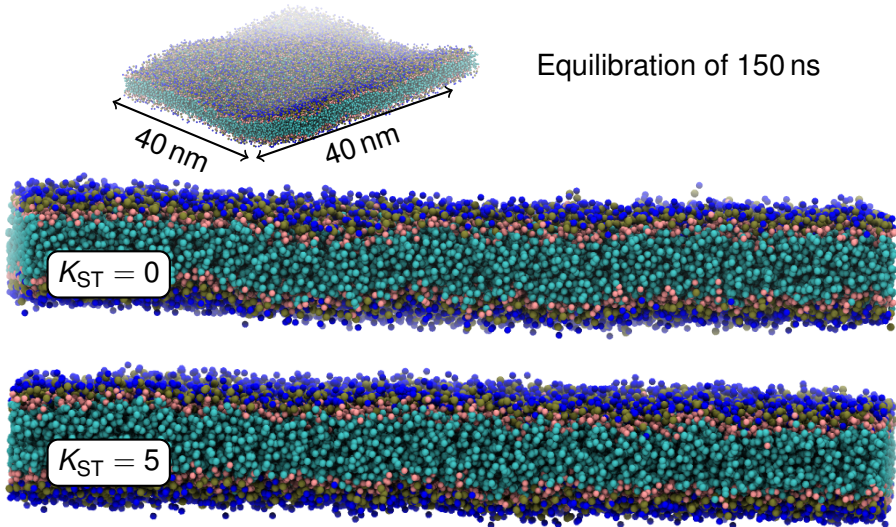
The effect of K_{ST} on DPPC-Bilayer

System setup



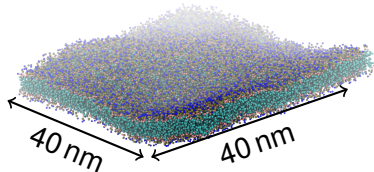
The effect of K_{ST} on DPPC-Bilayer

System setup

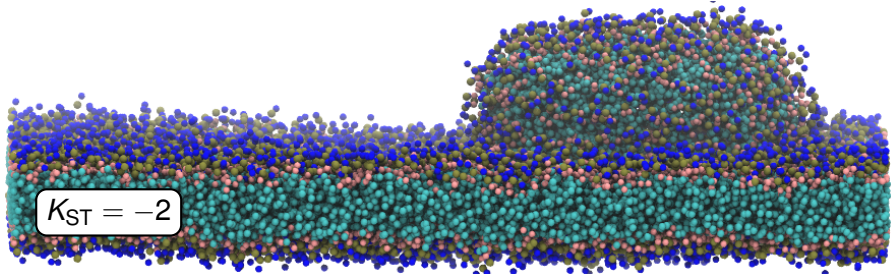


The effect of K_{ST} on DPPC-Bilayer

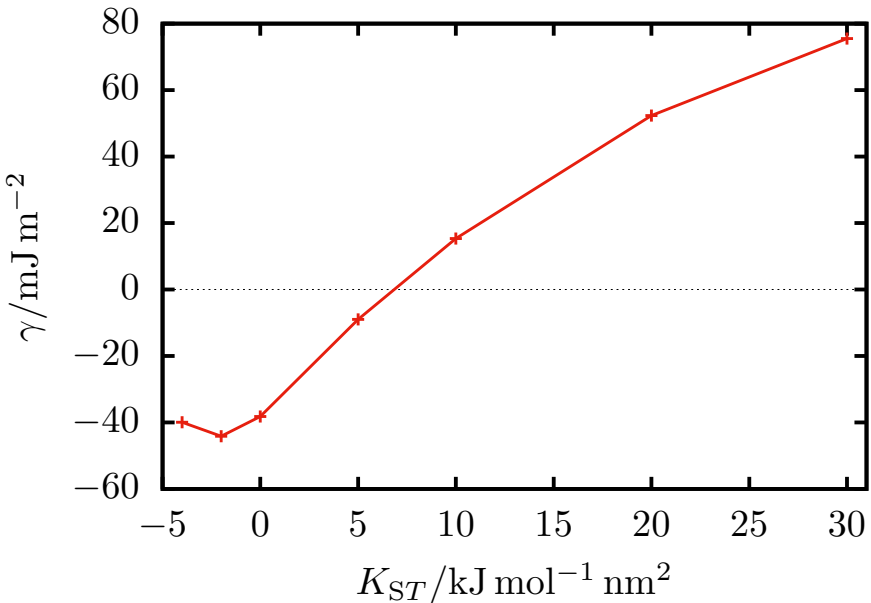
System setup



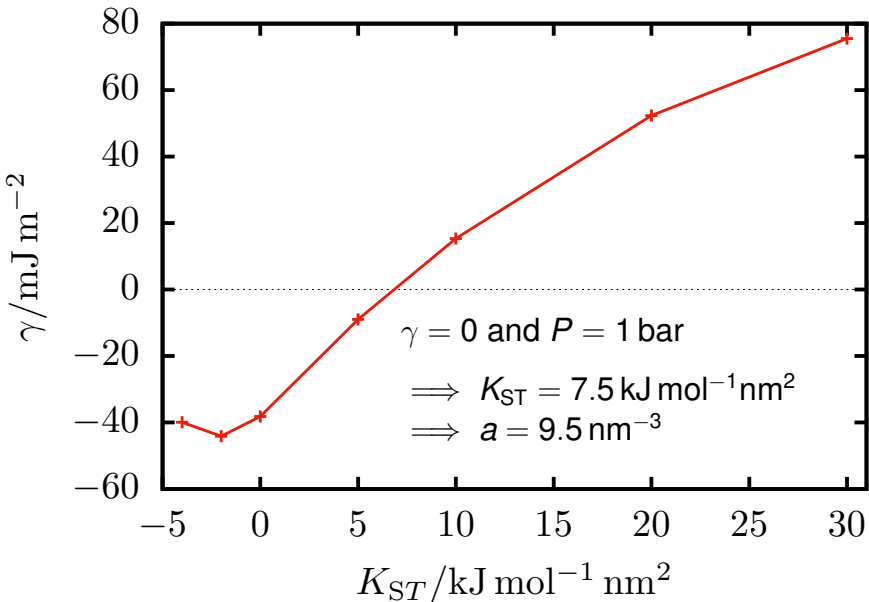
Equilibration of 150 ns



Tensionless condition: $\gamma = 0$

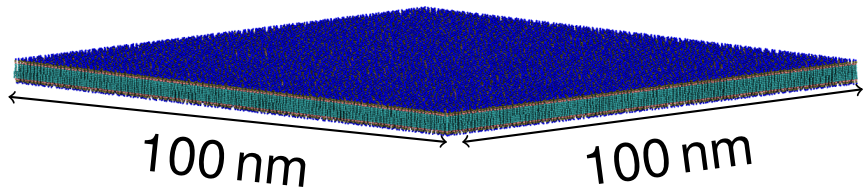


Tensionless condition: $\gamma = 0$



NPT-equilibration of Large lipid bilayers

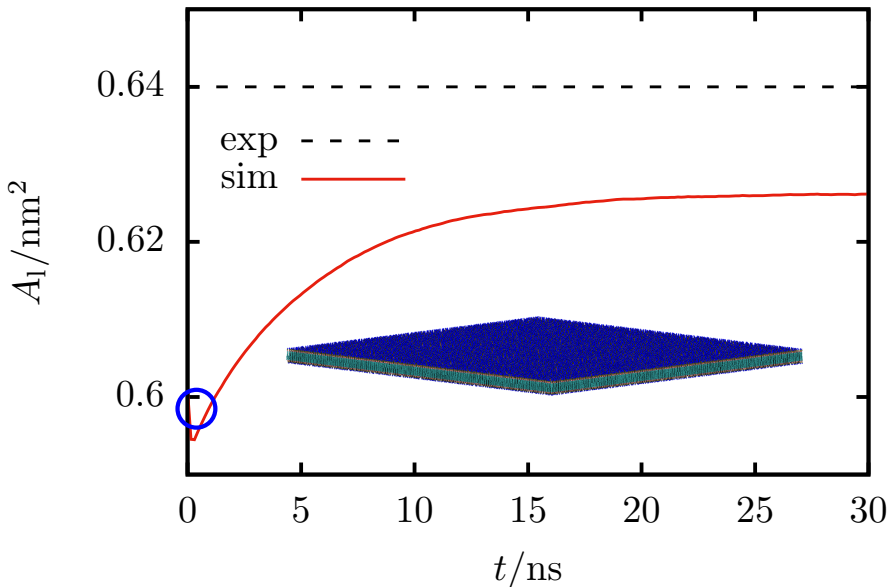
Initial configuration



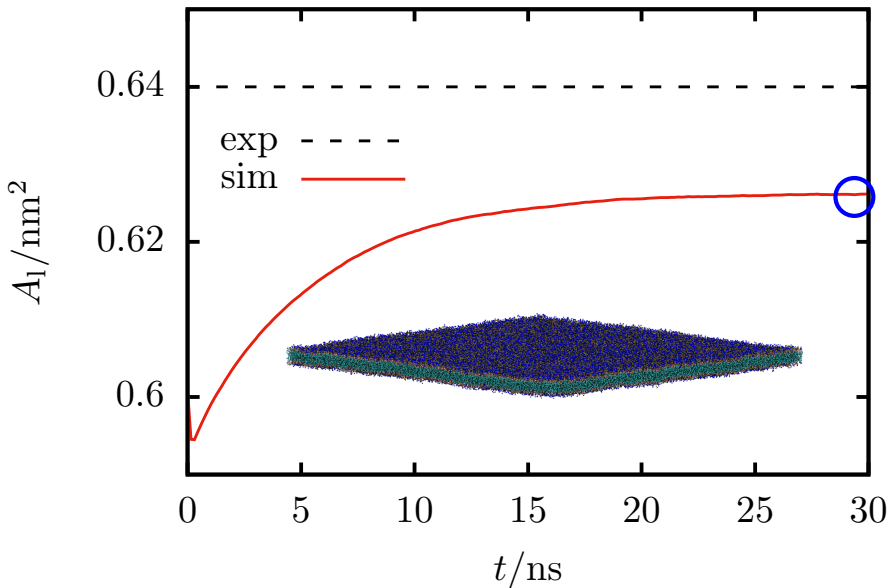
Lipids and solvent: 1.2 Million beads

~ 14 million atoms

NPT-equilibration of Large lipid bilayers



NPT-equilibration of Large lipid bilayers



Outlook

Parametrization:

- ▶ Avoid double counting
- ▶ Undulations
- ▶ Area-fluctuations

Outlook

Parametrization:

- ▶ Avoid double counting
- ▶ Undulations
- ▶ Area-fluctuations

Poster by Morten Ledum:



Machine learning optimization of hybrid particle-field model parameters

Morten Ledum¹, Sigrunn Lohndal Bone¹, Michele Cuscela¹, and Jürgen Gaus¹
¹Department of Chemistry and Biocenter Center for Quantum Molecular Sciences, University of Oslo, Norway
Institut für Physikalische Chemie, Johannes Gutenberg University, Mainz, Germany



Hylleraas

Abstract

The hybrid particle-field molecular dynamics method (hMP-MD) is an efficient alternative to standard particle-based coarse grained approaches. hMP-MD bypasses time-consuming and computationally expensive calculations by stratifying a system composed of non-interacting particles, coupled to an external field determined by the system. Explicit calculation of the field is avoided, which makes it easier to parallelize, leaving for excellent scaling in parallel implementations. Unfortunately, a general, robust protocol for finding the best set of parameters for the hMP model is today still missing. Here, we propose a machine learning approach based on Bayesian optimization that can achieve accurate hMP parameterizations with significantly fewer simulations than a standard model biological phospholipid bilayer.¹ We optimize $F(x)$, where x are the three free parameters and F is a function that measures the difference between the electron density profiles of hMP stratifications and reference coarse grained MD simulations using the MARTINI force field².

Bayesian optimization

The Bayesian optimization technique is suited for expensive black-box functions where derivatives are hard or impossible to compute. It combines a Gaussian process prior with a likelihood function to find the best point for picking out areas in parameter space where optimal parameters are likely to be found. The optimal experimental exploration strategy guides the search for the global minimum. The posterior variance of the variance is high, or the GP believes that the value of the underlying true objective is high.

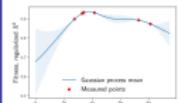


Fig. 2: ID example GP mass after 6 samples of the χ_{SP} parameter for a DMPC membrane.

Conclusions and outlook

A general, systematic technique for optimizing hMP parameters has been developed. The machine learning procedure, performing much better with or better than the hand-optimized reference parameterization in our chosen fitness metric, c.f. Tab. 2. The simple examples presented here demonstrate the potential of the optimization of the entire χ -matrix and other relevant simulation parameters.

However, the optimization scheme on the recently developed hybrid particle-field method with electrostatics is of particular interest.

References

- ¹G. Milos and T. Kowalewski, *The Journal of chemical physics* 100, 1000 (1994).
- ²J. Gaus, D. E. Collings, and F. C. Dean, *"How the bayesian optimization algorithm?", in Proceedings of the 1st annual conference genetic and evolutionary computation (Morgan Kaufmann Publishers Inc., 1999), pp. 325–332.*
- ³J. Martínez, H. J. Blasiuska, S. Nofman, D. P. Tieleman, and T. S. Deamer, *The journal of physical chemistry B* 113, 7880–7891 (2009).
- ⁴A. De-Nivola, Y. Zhou, T. Kowalewski, D. Reesmans, and G. Milos, *Journal of chemical theory and computation* 7, 2842–2860 (2011).

Phospholipid bilayer

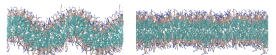


Fig. 1: Hybrid particle-field simulation of dipalmitoylphosphatidylcholine (DPPC) at parameters from the optimisation (left), and close to the optimal parameters (right).

Hybrid particle-field

The interaction energy $W(T)$ is assumed to depend only on the system temperature T through the density $\rho(r)$: $W(T) = W(0)(T)$.

$$W(T) = \int \left[\frac{k_B T}{2} \sum_{\alpha\beta} \nabla \phi_\alpha \cdot \nabla \phi_\beta \delta(r) \rho_\alpha(r) \rho_\beta(r) + \frac{1}{2\pi} \left(\sum_{\alpha} \rho_\alpha(r) - 1 \right)^2 \right].$$

The mean field potential at r for particle species K is

$$\psi_K(r) = k_B T \sum_{K'} \frac{\lambda_{KK'}}{k_B} \nabla \phi_K \cdot \nabla \phi_{K'}(r) + \frac{1}{k} \left(\sum_{K'} \rho_K(r) - 1 \right),$$

where $\lambda_{KK'}$ is interpreted as the MARTINI model $K-K'$ Lennard-Jones γ parameter.

Membrane profiles

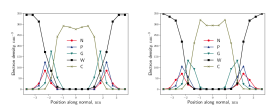


Fig. 3: Electron density profile across a DMPC membrane in MARTINI simulation (left) and hybrid particle-field simulation (right).

Parameterization fitness

Tab. 2: Coefficient of determination R^2 for simulations with the current machine learning parameterization compared with the reference hand-optimized parameterization. The first column indicates if a hMP coarse-grained molecular dynamics simulation with the MARTINI force field.

	MARTINI	hMP	hMP	
current	0.956	0.857	0.834	0.953
reference	0.904	0.735	0.999	0.785
improvement	3.9%	22.3%	1.05%	36.6%

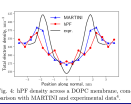


Fig. 4: hMP density across a DOPE membrane; comparison with MARTINI and experimental data³.

Acknowledgements

The authors acknowledge the support of the Norwegian Research Council through the CoE Hylleraas Center for Quantum Molecular Sciences (Grant 1.2019-2023), the Shaping the Future Research Program (2009-2013), Grant No. 2010-00001, and the Deutsche Forschungsgemeinschaft (DFG, German Research Foundation), project number 258300905 – TRR 186.

Acknowledgements

University of Oslo, Norway:

Michele Cascella

Hima Bindu Kolli

Morten Ledum

Victoria Ariel Bjørnestad

Reidar Lund



OCCAM
Molecular Dynamics

The logo for Hylleraas, consisting of two overlapping circles (one blue, one red) and the word "Hylleraas" in a bold, black, sans-serif font.

Yamagata University, Japan:

Giuseppe Milano

Antonio De Nicola

Tsudo Yamanaka

Sendai University, Japan:

Toshihiro Kawakatsu



The logo for the University of Oslo (UiO), consisting of the letters "UiO" in a large, black, sans-serif font, with a red dot to the right.